PERGAMON

Applied Radiation and Isotopes 56 (2001) 223–230

Applied Radiation and Isotopes

www.elsevier.com/locate/apradiso

A dual-compensated cryogenic microcalorimeter for radioactivity standardizations

R. Collé*, B.E. Zimmerman

Physics Laboratory, National Institute of Standards and Technology, Bldg 245, Room C114 Gaithersburg, MD 20899-8462, USA

Abstract

Efforts are underway by our laboratory to develop a microcalorimeter that can be routinely used for radioactivity standardizations of nuclides that decay by pure β-emission or by low-Z electron capture. The prototype calorimeter consists of a cryostat with two temperature-controlled stages and a base stage that are operated at nominal temperatures of 8 K. A unique aspect of the calorimeter's design is the ability to repeatedly engage and disengage the radioactive source from the second stage heat path using a magnetically activated elevator. The measurement of the total power from a radioactive sample is obtained from the difference in the second stage power with and without the source in place. As a result of extensive performance evaluations using ^{90}Sr–^{90}Y and ^{32}P brachytherapy seeds as well as with an internal calibration heater, many initial design flaws have been identified and are being addressed. Published by Elsevier Science Ltd.

Keywords: Brachytherapy; Calorimetry; Cryogenics; Instrument; Measurement; Metrology; Microcalorimetry; Radioactivity; Standards

1. Historical introduction and motivation

Classical calorimetric methods for the measurement of radioactivity have been in use for nearly a century. The first by Curie and Laborde (1903) verified that the heat produced by radioactive substances like radium and its decay products was due to the absorption of their radiations. Within a year, Curie and Dewar (1904) were utilizing cryogenic calorimeters at liquid-air and liquid-hydrogen temperatures, and Rutherford and Barnes (1903, 1904) were using twin-cup and differential calorimeters. These early studies, and those by many other contemporaneous researchers, were primarily concerned with characterizing the amount of heat produced from various nuclides in the naturally occurring decay series and from radioactive minerals. The apogee in radionuclidic calorimetry was probably the determination by Ellis and Wooster (1925) that the maximum energy and average energy of the β-radiation from ^{210}Bi were different, which bore out the need for the neutrino hypothesis. Since calorimetry requires the use of samples having rather large quantities of radioactivity, it has, for the past 25 years or so, been used mainly for the assay of tritium and special nuclear materials in the nuclear-power and -weapon industries and for fusion technology [cf. ANSI (1987) and Anderson (1992)]. Our laboratory's current reinterest in the use of calorimetry for radionuclidic metrology derives directly from the need to provide standardizations for rather large, GBq-range, pure-β-emitting, brachytherapy sources (Collé, 1999). Calorimetry may provide an alternative method for the calibration of such sealed sources that normally require destructive assays.

Reviews of the radionuclidic calorimetry literature are available, although none are recent. Myers (1949), in an exhaustive review, compiled a very comprehensive bibliography. A somewhat-less-detailed encyclopedic article by Mann (1962) extended the references to 1958 and summarized the various classes of calorimeters in use. The most recent survey—an excellent one, but sadly

*Corresponding author. Tel.: +1-301-975-5527; fax: +1-301-926-7416.

E-mail address: rcolle@nist.gov (R. Collé).

0969-8043/02/$ - see front matter Published by Elsevier Science Ltd.
PII: S0969-8043(01)00192-0

Table 1
Power P (in units of μW) per unit activity A (in units of GBq) for various nuclides having an average energy per decay of $\hat{E}$

Nuclide	Decay mode	$\hat{E}$ (MeV)	P/A (μW GBq^{-1})
^{3}H	β	0.00569	0.912
^{55}Fe	EC	0.00567	0.908
^{103}Pd	EC	0.0565	9.05
^{125}I	EC	0.0588	9.42
^{63}Ni	β	0.0174	2.79
^{14}C	β	0.0495	7.93
^{33}P	β	0.0764	12.2
^{32}P	β	0.695	111.0
^{90}Sr	β	0.196	31.4
^{90}Y	β	0.934	150.0
^{226}Ra (to ^{210}Pb)	α/β chain	—	4340.0[a]
^{210}Pb subseries	α/β chain	—	935.0[a]

[a] Per GBq of the parent.

now nearly 30 years old—by Ramthun (1973) addresses, more specifically, the metrological aspects of calorimetry as applied to radioactivity.

The presently described work is this laboratory's second foray into radionuclidic microcalorimetry. For nearly 40 years, starting in 1953, the distinguished Wilfrid B. Mann and collaborators in the Radioactivity Group at the National Institute of Standards and Technology (NIST)—formerly called the National Bureau of Standards (NBS)—utilized a twin-gold-cup, Peltier-effect microcalorimeter for a great variety of studies (Mann, 1973; Mann and Unterweger, 1995). Mann's microcalorimeter (Mann, 1954) was an adaptation of the "radiobalance" of Callandar (1910).

In terms of the use of calorimetry for radioactivity standardizations, the underlying assumption is that the calorimeter will absorb (i.e., and measure) all or a known part of the radiation. The basic relationship for the rate of energy (or heat) input, or power P, and the activity A of a radioactive source contained in the calorimeter is

$$P = kA\hat{E}, \tag{1}$$

where $\hat{E}$ is the average energy per decay for the radionuclide and k is a calibration factor that relates the fraction of the total power from radioactive decay that is dissipated in the calorimeter. If all of the radiation is absorbed (and measured), then $k = 1$. Table 1 summarizes the power per unit activity for a variety of nuclides.

2. The microcalorimeter and its operation

The prototype microcalorimeter, currently undergoing development for routine use, is unique, and was initially designed and constructed by Science Research Laboratories, Inc. (Cambridge, MA) under a NIST-sponsored contract. An overview of the component parts of this calorimeter is illustrated in the schematic of Fig. 1. The original unit was based, in part, on an earlier design for an in-beam-line cryogenic neutron calorimeter (Richardson et al., 1991, 1998), and has been previously described in detail by Richardson (1999, 2000). Therefore, only a very brief description will be given here. Fig. 2 illustrates the microcalorimeter's principles of operation. Refer to the caption for details. The microcalorimeter consists of a cryostat with two temperature-controlled stages and a base stage that are operated at nominal temperatures of 7.5–8.0 K within a vacuum chamber (maintained at about 10^{-5} Pa). The stages are connected through weak thermal links and operate at temperatures that are separated from each other by about 0.1 K. Cooling is provided by a He closed-cycle mechanical refrigerator whose coldhead to the cryostat was subsequently found to require auxiliary air cooling and whose compressor was also found to need a separate temperature-controlled cooled-water chiller to obtain a reasonably constant base temperature below 8 K. The temperature of each of the compensated stages is very sensitively monitored with Ge-resistor thermometers and controlled through a power-feedback control loop using a simple bridge circuit. Temperature control on each stage is effected with resistance heaters whose power is measured to better than 0.1% using precision "shunt" resistors. In addition to the two controlled stages, the base temperature of the cryostat is continually monitored by a voltage measurement with an approximately calibrated diode thermometer which is driven with a 10 μA constant current source. The base temperature measurements are only used for monitoring the system conditions, e.g., during the calorimeter cooldown phase or during stage-two power measurements. The calorimeter's temperature control and power measurement circuitry operates under a LabVIEW (National Instruments Corp., Austin, TX) software environment. Fig. 3 contains additional details and a description of the second stage circuitry. The hard-wired bridge set points are very sensitive, such that the second stage compensation (and P_2 power measurement) will not "lock" into control (or will go out of control) if the base temperature rises above about 7.9 K.

Measurements are effected by containing the radioactive source inside a suitable source holder that can absorb all (or a well-determined fraction) of the total ionizing radiation energy, and mounting the source on a magnetically activated elevator that can be coupled and decoupled to the second stage platform. Obviously, the assembly of the source holder on the elevator must occur before the cryostat is reassembled, evacuated, and cooled. The ability to repeatedly engage and disengage the radioactive source from the second stage heat path

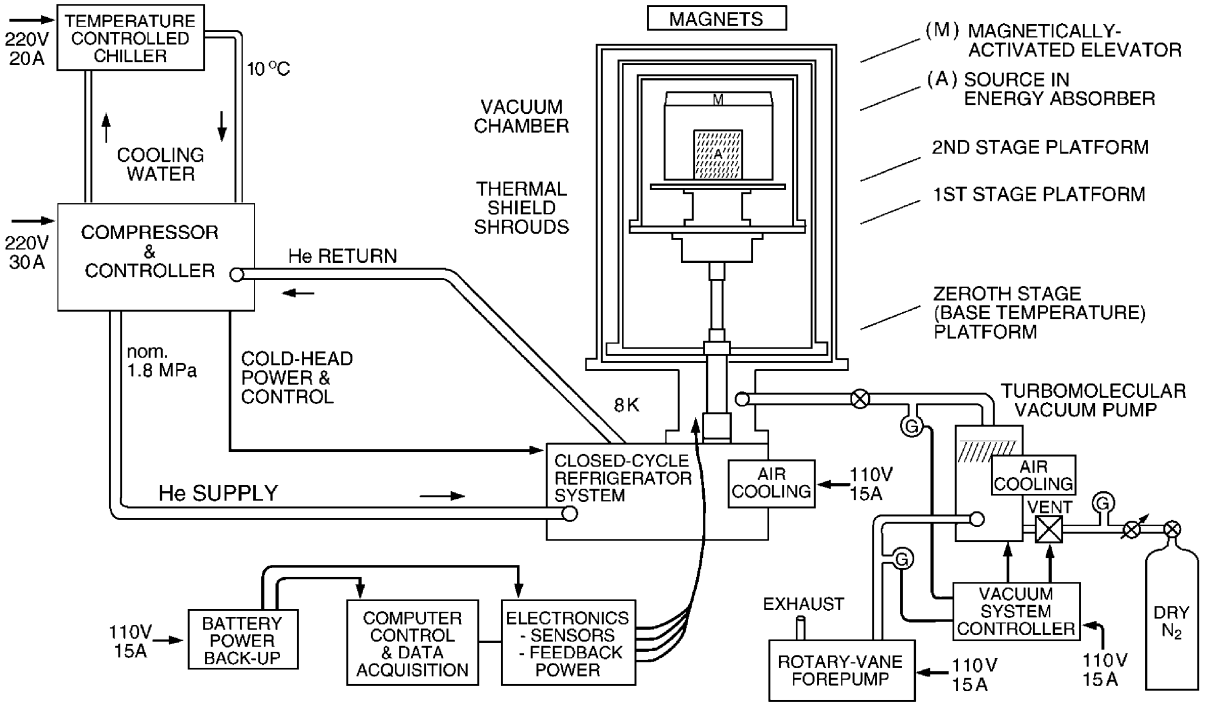

Fig. 1. Overview of the microcalorimeter's layout and all of its component parts.

through the use of permanent magnets (that can do no work and therefore expend no power to the system) is a unique aspect of the calorimeter's design. The measurement of the total power P_A from a radioactive sample is obtained from the difference $[P_{2(out)} - P_{2(in)}]$ in the second stage power with $(P_{2(in)})$ and without $(P_{2(out)})$ the source in place. When the source (and elevator) is disengaged from the second stage platform it becomes thermally coupled to the first stage at the top of its thermal shield shroud. Using the notation in Fig. 2, the second stage power, under the two positions, is given by

$$P_{2(out)} = p_{21(out)} + p_{loss(out)} - P_A \quad (2)$$

and

$$P_{2(in)} = p_{21(in)} + p_{loss(in)}, \quad (3)$$

which yields

$$P_A = [P_{2(out)} - P_{2(in)}] - \Delta P \quad (4)$$

and where the error term ΔP is given by

$$\Delta P = [p_{21(out)} - p_{21(in)}] + [p_{loss(out)} - p_{loss(in)}] \quad (5)$$

is, hopefully, negligibly small. Assuming that there are no ionizing radiation losses (that might otherwise result from incomplete energy absorption in the source holder) that contribute to p_{loss}, then the error will be exactly equal to $\Delta P = 0$ if the two stage temperatures T_2 and T_1 remain perfectly constant under "perfect" power-compensation control. In this case, the thermal radiation contribution to p_{loss} and the power p_{21} through the weak link will be exactly equal for both the "in" and "out" source positions. In the absence of this ideality, one might expect there to be a slight temperature increase in T_1 and decrease in T_2 in positioning the "hot" source from the second stage platform to the first stage shroud. The result of such temperature shifts on ΔP can be expected to be somewhat compensatory since they would have the effect of decreasing p_{21} while increasing the thermal radiation part of p_{loss}.

3. Performance evaluation results

The calorimeter has been undergoing extensive evaluations and design modifications since August 2000. Numerous preliminary measurements have been performed using both ^{32}P and ^{90}Sr–^{90}Y brachytherapy seeds, as well as with an internal calibration heater (mounted on the elevator) whose input power can be varied. The heater power is accurately measured with shunt-resistor circuitry that is similar to that used to determine P_2.

Table 2 contains some typical results obtained with both the calibration heater at several power levels and

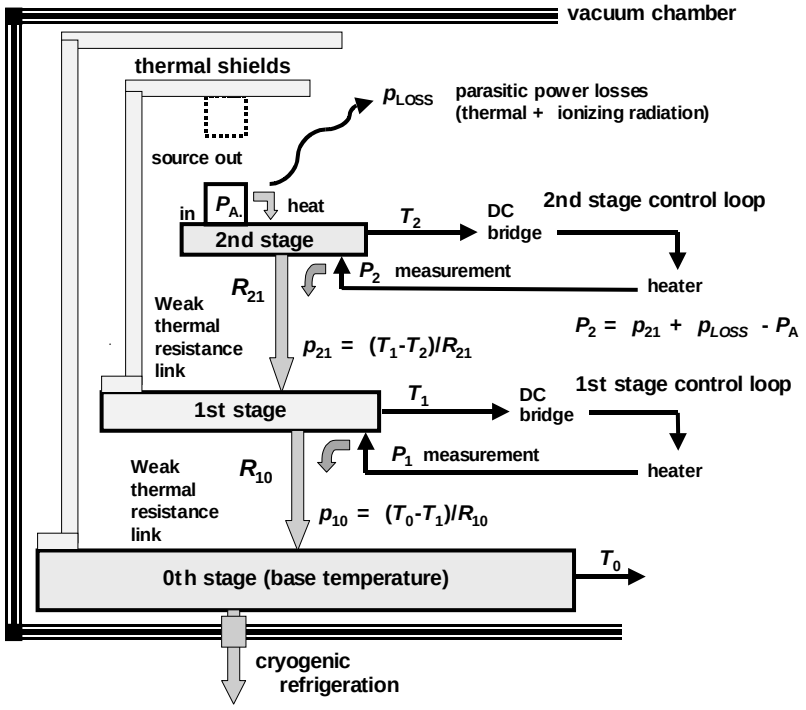

Fig. 2. Schema illustrating the calorimeter's main components and operating principles for its dual-compensation method. The three stages all operate at nominal temperatures of 7.5–8.0 K and are connected through two weak thermal resistance links R_{21} and R_{10}. They are monitored and heat-compensated through the control loops such that the first stage temperature T_1 is controlled to 1–5 mK variations while the second T_2 is controlled to within 10–50 μK variations. With the source (having a power P_A) engaged on the second stage, the feedback power is $P_2 = (p_{21} + p_{loss} - P_A)$, where $p_{21} = (T_1 - T_2)/R_{21}$ is the power through the weak link (which remains constant so long as T_1 and T_2 remain constant) and where P_{loss} is any parasitic power loss (due to either second stage *thermal* power losses to the first stage thermal shield surfaces or to escaping *ionizing radiation*).

three replicate measurements of a 175 MBq ^{90}Sr brachytherapy source. Fig. 4 illustrates the temporal response of the calorimeter to the calibration heater in the source "in" and "out" positions for an applied power of 16.50 μW. Data of comparable kind for a 140 MBq ^{90}Sr source are shown in Fig. 5. The ^{90}Sr–^{90}Y sources (Collé, 2000) used for these measurements were contained in threaded brass source holders (that were somewhat irregularly shaped, right-circular cylinders having an approximate 16 mm outer diameter, 14 mm height, and with wall thickness ranging from 4 to 6 mm) that were mounted on the elevator. The holders are not optimal (see Section 4 below). They were originally designed to contain ^{125}I seeds, and were only used because they were conveniently available.

To date, the system has been able to make measurements with a standard uncertainty of only about 2–3% in the range of 25 μW. Even this precision is attainable only if one performs sufficient replicate measurements. The stability of the instrument is quite erratic, and exhibits large transients and long-term drifts in the second stage power, whose causes are poorly understood. Short-term (<0.5 d) baseline stability is typically not much better than ± 1 μW. Demonstrated long-term stability over several days, which is necessary to establish the ΔP_2 difference, is, at present, only about ± 5 μW. This overall performance is roughly an order-of-magnitude worse than expected from design principles (Richardson, 1999, 2000). In addition, there is some evidence suggesting that there are parasitic heat losses from the elevator (and source holder) surfaces to the first stage thermal shield, and evidence to suggest that the time-constants associated with the reestablishment of thermal steady states in the calorimeter after changes in the elevator position are sometimes very inconsistent. The former may arise from poor thermal conduction in the second stage heat path due to poorly conducting oxidized-aluminum surfaces (as well as the size of the elevator structure relative to the stage platforms), while the latter may arise because of problems with the thermal coupling and uncoupling of the source-elevator to the second stage or first stage shroud. As a result of our systematic investigations, many potential design

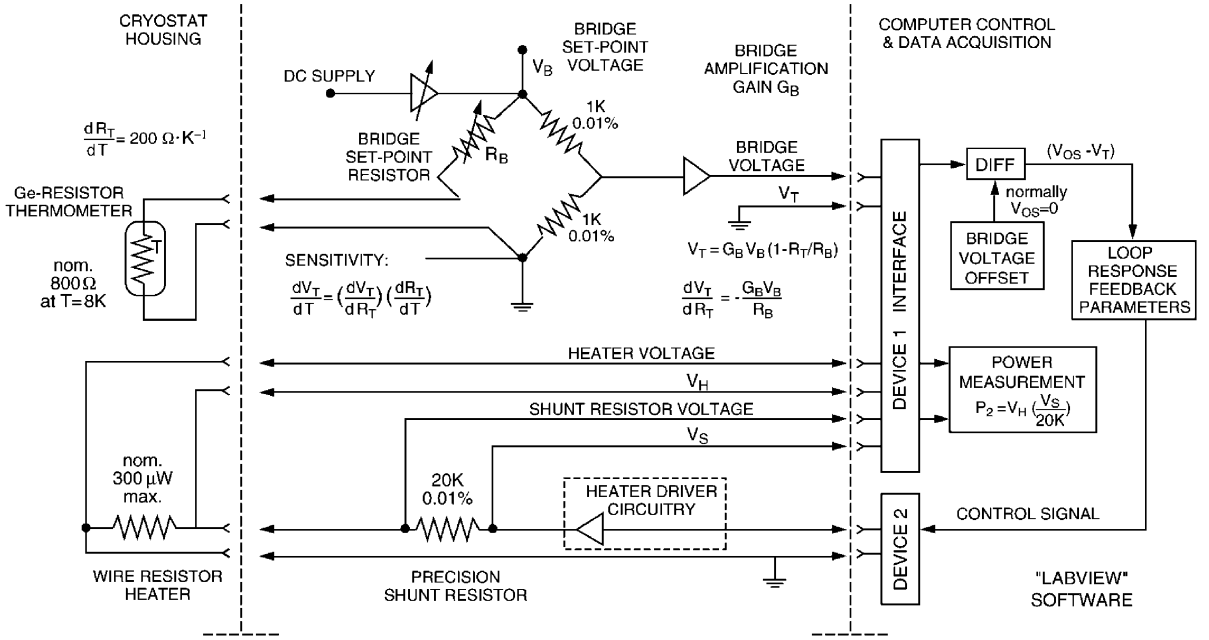

Fig. 3. Schema of the calorimeter's second stage temperature-monitoring and -controlling circuitry, including the high-gain Ge-resistor thermometer (having a sensitivity dR/dT of nominally $200\,\Omega\,K^{-1}$ at 8 K) and DC bridge (whose gain G_B results in a bridge-voltage output sensitivity dV_T/dT of about $400\,mV\,K^{-1}$), the computer-controlled feedback control loop, and the heater's feedback power measurement P_2 which is obtained from very accurate measurements of the heater voltage V_H and the voltage V_S across a precision 20 kΩ shunt resistor. For $P_2 = 10\,\mu W$, the V_H and V_S voltages are on the order of 0.5 V which can readily be measured with a precision within $\pm 0.01\%$ and with an accuracy of better than 0.1%.

Table 2
Microcalorimeter performance evaluations: (a) comparing the applied power P_A of the calibration heater to the measured difference ΔP_2 in the second-stage feedback power for the "in" and "out" source positions; and (b) replicate power measurements on a nominal 175 MBq ^{90}Sr source[a]

	P_A (μW)	ΔP_2 (μW)	$\Delta P_2/P_A$
Calibration heater	16.50	16.9 ± 0.6	1.024 ± 0.036
	16.50	16.3 ± 0.4	0.988 ± 0.024
	16.51	16.6 ± 0.9	1.005 ± 0.055
	28.03	26.2 ± 1.4	0.935 ± 0.050
	30.00	30.8 ± 0.7	1.026 ± 0.023
	49.90	46.6 ± 2.9	0.930 ± 0.058
		Mean	0.985 ± 0.017
^{90}Sr–^{90}Y seeds (nominal 175 MBq)	32 (nominal)	32.8 ± 1.2	
		29.1 ± 0.9	
		30.5 ± 1.0	
	Mean	30.8 ± 1.1	

[a] The uncertainty in the calibration heater's applied power P_A is negligible ($< 10^{-3}\%$) with respect to that for ΔP_2. The uncertainty interval on each measured ΔP_2 value represents only the propagated standard deviation obtained from the precision in the P_2 measurements for the "in and out" source positions. The tabulated uncertainty on each of the two mean values is a standard deviation of the mean.

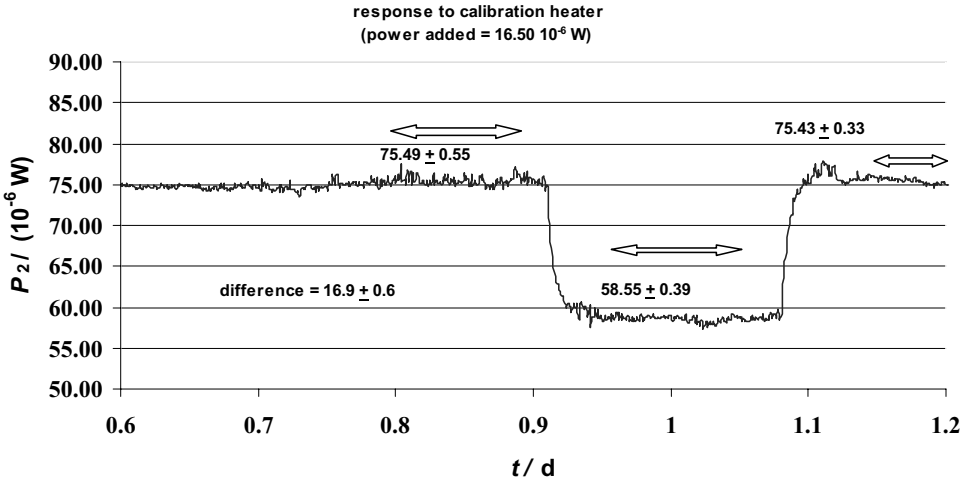

Fig. 4. Response of the microcalorimeter to the calibration heater in terms of the measured second stage feedback power P_2 (in units of μW) as a function of time t (in units of days). The upper and lower plateaus at about 75 and 59 μW correspond to the source "out" (elevator up) and "in" (elevator down) positions, respectively.

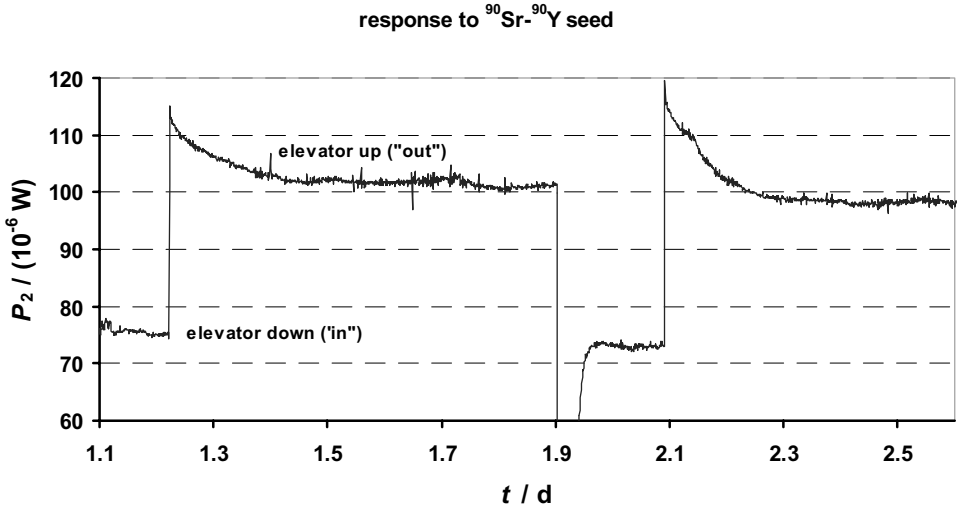

Fig. 5. Measurement of the power from ^{90}Sr–^{90}Y brachytherapy seeds (having a nominal activity of 140 MBq ^{90}Sr) with the microcalorimeter as obtained from the difference in the second stage feedback power (nominally $\Delta P_2 = 25\,\mu W$) in the source "in" and "out" positions.

flaws have been identified and are being addressed (see Section 5).

4. Modeling results

Monte Carlo modeling simulations for possible photon losses from source holders as mounted in the calorimeter are also being performed. Our intent is to use these calculations to optimize designs of suitable energy-absorbing sample holders (unique for each radionuclide and source geometry) as well as to obtain corrections for possible losses. Table 3 provides some typical results obtained for the small brass holder that was used to measure the ^{90}Sr–^{90}Y seeds. As indicated, the power loss (even in this non-optimal holder) was estimated to be about 0.8%. These calculations were carried out using the EGS4 radiation transport package, along with its DOSRZ user code (Nelson et al., 1985). For modeling purposes, the geometrical configuration of the microcalorimeter was simplified, but this geometry was specified with sufficient detail as to allow the

Table 3
Results of Monte Carlo calculations for the fractional distribution (in percent) of the power P_A in the modelized calorimeter for a ^{90}Sr–^{90}Y source in the "in" and "out" positions[a]

	Source "in"	Source "out"
Brass source holder	>99.15(+)	>99.17
Elevator	0.03(+)	0.02
Second stage base	0.04(+)	0.04(−)
First stage shroud	0.02	0.01
Escaped	<0.76	<0.76
Fraction of P_A in P_2 measurement	>99.18	

[a] The statistical uncertainty (in terms of a relative standard deviation) in the calculations for the *total* power deposition (i.e., for the total number of events scored) is 0.3%. The uncertainty in regions having very small power depositions can, therefore, be as large as 100% or more. There are essentially no differences in the calculated results for the two positions.

deposited energy from the ^{90}Sr–^{90}Y source to be scored in each of the important regions of the instrument.

Eventually, we plan to extend our modeling for the heat transport in the calorimeter in order to perhaps better understand the causes of the present baseline instabilities, as well as to optimize the microcalorimeter's design and performance.

5. Future directions

Efforts are underway to drastically improve the operating performance of the microcalorimeter so that it can become usable for routine standardizations. Several enhancements have already been incorporated, including much greater stabilization in the base stage temperature as a result of improving the cryostat vacuum and in controlling the air- and water-cooling to the He refrigerator's compressor and coldhead. The improved evacuation may also have helped to minimize power variations due to residual gas loading. Greater efforts were also made to minimize thermal conduction along the calorimeter's internal wiring. Many other avenues are under investigation. We are actively considering providing the base stage with a control-loop heater which would be similar to that used on the two upper stages. The Ge-resistor sensors used in the first and second stage control loops are resistant to ionizing radiation, but we have discovered that they are not recommended for use in "strong magnetic fields". We are evaluating whether the relatively strong SmCo magnets incorporated into the source-holder elevator are a source of the system instability. Richardson (2000) has also speculated that these magnets may be a suspect source of exothermic phase changes. The most substantial change that is underway involves the complete redesign of the elevator and source-holder system. Our goal is to devise a new elevator configuration which (i) will have better conductivity and thermal coupling to the second stage platform and to the first stage shroud (in the "up" position), (ii) will be substantially smaller in volume to minimize parasitic heat losses between the stages, and (iii) will utilize permanent magnets to move the elevator between positions, but be removable once the elevator is in place.

Lastly, to augment our capability to perform calorimetric standardizations, we have also recently acquired a commercial, temperature-regulated, isothermal microcalorimeter, which operates at near-ambient temperatures. Very preliminary results suggest that this calorimeter's baseline stability is about $\pm 0.1\,\mu W$ over short (<1 d) time intervals and about $\pm 1\,\mu W$ for long-term drifts. This is at least a factor of 5 better than that presently attainable with our cryogenic microcalorimeter. It is not, however, as good as the cryogenic calorimeter's design expectations. As a result, it is not yet apparent which calorimeter will be used for secondary confirmatory measurements and which will ultimately serve as our "primary" calorimetric calibration standard.

Acknowledgements

The National Institute of Standards and Technology (NIST) is an agency of the Technology Administration of the US Department of Commerce. Certain commercial equipment, instruments, and materials are identified in this paper to foster understanding. Such identification does not imply recommendation or endorsement by NIST, nor does it imply that the materials are the best available for the purpose. Dr. F.J. Schima (formerly of NIST) must be credited for championing the initial calorimeter development project, while Dr. J.M. Richardson (Science Research Laboratory) must also be acknowledged for his continuing advice and interest on the calorimeter's fate. The authors thank their NIST colleagues: Mr. S. Seltzer for his assistance in getting us on track with our Monte Carlo calculations, and Drs. L. R. Karam and B.M. Coursey for their enthusiastic support of this work.

References

Anderson, J.L., 1992. Tritium technology programs in the United States. Fusion Technol. 21, 226.

ANSI, American National Standards Institute 1987. Plutonium-Bearing Solids—Calibration Techniques for Calorimetric Assay, Report N15.22, ANSI, New York.

Callandar, H.L., 1910. The radio-balance. Proc. Phys. Soc. 23, 1.

Collé, R., 1999. Chemical digestion and radionuclidic assay of TiNi-encapsulated ^{32}P intravascular brachytherapy sources. Appl. Radiat. Isot. 50, 811.

Collé, R., 2000. On the radioanalytical methods used to assay stainless-steel-encapsulated, ceramic-based ^{90}Sr–^{90}Y intravascular sources. Appl. Radiat. Isot. 52, 1.

Curie, P., Laborde, A., 1903. Sur la chaleur dégagée spontanément par les sels de radium. Compte Rendu 136, 673.

Curie, P., Dewar, J., 1904. Discourse by Sir James Dewar on liquid hydrogen calorimetry. Proc. Roy. Inst. 17, 596.

Ellis, C.D., Wooster, W.A. 1925. The heating effect of the γ-rays of radium B and radium C. Philos. Mag. 50(6), 521; Note on the heating effect of the γ-rays of RaB and RaC. Proc. Camb. Philos. Soc. 22, 595.

Mann, W.B. 1954. A radiation balance for the microcalorimetric comparison of four national radium standards. J. Res. NBS 53, 277; Use of Callendar's "radiobalance" for the measurement of the energy emission from radioactive sources. J. Res. NBS 52, 177.

Mann, W.B., 1973. Radiactive calorimetry: a review of the work at the national bureau of standards. Nucl. Instrum. Methods 112, 273.

Mann, W.B., Unterweger, M.P., 1995. The NBS/NIST Peltier-effect microcalorimeter: a four-decade review. Appl. Radiat. Isot. 46, 185.

Myers, O.E., 1949. Calorimetric radioactivity measurements. Nucleonics 5 (11), 37.

Nelson, W.R., Hirayama, H., Rodgers, D.W.O., 1985. The EGS4 code system, SLAC Report 265, Stanford University, Palo Alto, CA.

Ramthun, H., 1973. Recent developments in calorimetric measurements of radioactivity. Nucl. Instrum. Methods 112, 265.

Richardson, J.M., 1999. A calorimeter for the nondestructive assay of tritium-contaminated samples. Phase II Final Technical Report prepared for the US Department of Commerce under Contract No. 50-DKNB-6-90163, Science Research Laboratory Inc., Cambridge, MA.

Richardson, J.M., 2000. A calorimeter for the nondestructive assay of tritium-contaminated samples. IEEE Trans. Nucl. Sci. 47, 854.

Richardson, J.M, Chupp, T.E., Robertson, R.G.H., Wilkerson, J.F., 1991. Nucl. Instrum. Methods A 306, 291.

Richardson, J.M, Snow, W.M., Chowdhuri, Z., Greene, G.L., 1998. Accurate determination of thermal neutron flux via cryogenic calorimetry. IEEE Trans. Nucl. Sci. 45, 550.

Rutherford, E., Barnes, H.T., 1903. Heating effect of the radium emanation. Nature 68, 622.

Rutherford, E., Barnes, H.T., 1904. Heating effect of the radium emanation. Philos. Mag. 7 (6), 202.